Am J Cancer Res 2021;11(11):5428-5439
www.ajcr.us /ISSN:2156-6976/ajcr0137804

Original Article

$CD11b^+DIP2A^+LAG3^+$ cells facilitate immune dysfunction in colorectal cancer

Chie Kudo-Saito[1], Yamato Ogiwara[1], Hiroshi Imazeki[1,2], Narikazu Boku[2], Yasushi Uemura[3], Rong Zhang[3], Akiko Kawano-Nagatsuma[4], Motohiro Kojima[5], Atsushi Ochiai[4]

[1]Department of Immune Medicine, National Cancer Center Research Institute, Tokyo, Japan; [2]Division of Gastrointestinal Medical Oncology, National Cancer Center Hospital, Tokyo, Japan; Divisions of [3]Cancer Immunotherapy, [4]Biomarker Discovery, [5]Pathology, Exploratory Oncology Research & Clinical Trial Center, National Cancer Center, Chiba, Japan

Received July 29, 2021; Accepted September 1, 2021; Epub November 15, 2021; Published November 30, 2021

Abstract: Colorectal cancer (CRC) is one of the most common malignant tumors worldwide, and tumor metastasis is the leading cause of death. Targeting immune inhibitory checkpoint inhibitory pathways has attracted great attention, since the therapeutic efficacy induced by the specific blocking antibodies has been demonstrated even in metastatic CRC patients. However, the clinical outcome is low in many cases, and thus more effective treatments are needed in the clinical settings. A SPARC family member follistatin-like 1 (FSTL1) is known as a key driver of tumor metastasis in various types of cancer. However, the immunological roles of the FSTL1 in the CRC pathogenesis remain to be elucidated. In this study, we investigated the molecular mechanisms underlying the refractory $FSTL1^+$ CRC using murine and human FSTL1-transduced CRC cells. Also, based on the results, we evaluated anti-tumor efficacy induced by agents targeting the identified molecules using murine CRC metastasis models, and validated the clinical relevancy of the basic findings using tumor tissues and peripheral blood obtained from CRC patients. FSTL1 transduction conferred EMT-like properties, such as low proliferative (dormant) and high invasive abilities, on tumor cells. When the transfectants were subcutaneously implanted in mice, $CD11b^+DIP2A^+LAG3^+$ cells were abundantly expanded locally and systemically in the mice. Simultaneously, apoptotic T cells increased and were lastly excluded from the tumor tissues, allowing tumor aggravation leading to resistance to anti-PD1/PDL1 treatment. Blocking FSTL1 and LAG3, however, significantly suppressed the apoptosis induction, and successfully induced anti-tumor immune responses in the CRC metastasis models. Both treatments synergized in providing better prognosis of the mice. FSTL1 was significantly upregulated in tumor tissues and peripheral blood of CRC patients, and the $CD11b^+DIP2A^+LAG3^+$ cells were significantly expanded in the PBMCs as compared to those of healthy donors. The expansion level was significantly correlated with decrease of potent $Ki67^+GZMB^+$ CTLs. These results suggest that the FSTL1-induced $CD11b^+DIP2A^+LAG3^+$ cells are a key driver of immune dysfunction in CRC. Targeting the FSTL1-LAG3 axis may be a promising strategy for treating metastatic CRC, and anti-FSTL1/LAG3 combination regimen may be practically useful in the clinical settings.

Keywords: Colorectal cancer, metastasis, FSTL1, DIP2A, LAG3, tumor evasion, immune dysfunction

Introduction

Colorectal cancer (CRC) is one of the most common malignant tumors worldwide, and tumor metastasis is the leading cause of death [1]. Exploration of the molecular mechanisms underlying cancer metastasis has been intensively conducted especially focusing on epithelial-mesenchymal transition (EMT) and the associated cancer stem cells [2]. However, the scientific advances have not necessarily led to the practical advances, and thus the median overall of the patients with unresectable metastatic CRC is still only 30 months in clinical settings [3]. Targeting immune inhibitory checkpoint (IC) pathways has attracted great attention as a promising strategy for treating metastatic CRC, since treatment with the specific blocking mAbs, such as anti-CTLA4 mAb and anti-PD1/PDL1 mAbs, are effective even in metastatic cancer, including CRC. However, the therapeutic efficacy is limited to a part of the

patients having tumors with PDL1 expression, microsatellite instability (MSI), and mismatch repair deficiency [4-6]. To improve the present status, antibodies targeting other IC molecules, such as LAG3 and TIGIT, have been clinically developed in combination with other agents in many clinical trials [7, 8]. However, the clinical evaluation is still underway, and more effective treatments are urgently needed in the clinical settings.

In cancer metastasis, a member of the SPARC family follistatin-like 1 (FSTL1) is known as a key molecule regulating the cancer EMT, and significant correlation with poor prognosis of patients has been demonstrated in a variety of cancer, including esophageal cancer [9], hepatocellular carcinoma [10], lung cancer [11], glioblastoma [12], and CRC [13, 14]. However, the immunological roles of the FSTL1 remain to be elucidated in the CRC pathogenesis. Understanding both tumor cells and host immunity is important for treating refractory cancer, since tumor biological and immunological heterogeneity are produced by interplays between them [15, 16]. In this study, we investigated the immunological mechanisms underlying refractory FSTL1^{+} CRC using murine and human FSTL1 transfectants to clarify the influences of FSTL1, mouse CRC metastasis models, and clinical samples obtained from CRC patients, and attempted to establish an effective treatment regimen that could be practically applicable to clinical therapy of metastatic CRC.

Materials and methods

Mice and cell lines

Five-week-old female C57BL/6 and BALB/c mice were purchased from Charles River Laboratories (Japan), and were maintained under pathogen-free conditions. The mice were used according to the protocols approved by the Animal Care and Use Committee at the National Cancer Center Research Institute. Murine CRC cell lines (MC38 and Colon26) were purchased from Cell Resource Center for Biomedical Research at Tohoku University in Japan, and human CRC cell line HCT116 cells were purchased from ATCC in US. The cells were expanded and frozen in liquid nitrogen to avoid changes occurred by a long-term culture until use after confirming the mycoplasma negativity using a Hoechst-staining detection kit (MP Biomedicals). The cells were cultured in 10% FBS/DMEM (GIBCO), and were trypsinized and washed in MEM (GIBCO) before use in experiments.

Establishment of FSTL1 transfectants

Murine FSTL1$^{-/low}$ MC38 cells were transfected with recombinant lentiviruses encoding murine *fstl1* (GenBank accession number: NM_008047) or none as mock transfection as described before [17]. Human FSTL1$^{-/low}$ HCT116 cells were transfected with a plasmid vector pCMV6-ENTRY (Origene Technologies) encoding human human *fstl1* (GenBank accession number: NM_007085), or the empty vector as mock transfection by electroporation (0.4 kV, 25 μFD). The transfectants were cultured in 10% FBS/DMEM with G418 (ThermoFisher). The transduction efficacy was evaluated by RT-PCR and ELISA (1×10^5 cells/10 ml/3 days) as described before [18].

Functional analysis of tumor cells

Tumor functions were assessed as described before [19]: Cell proliferation (2 days) by WST1 assay (Takara), cell adhesion (2 hour) using fibronectin-coated multiwell plates (Corning), and cell invasion (4 hours) using a transwell chamber with a matrigel-coated membrane (Corning). Tumor cells (5×10^5 cells) were subcutaneously (s.c.) implanted in mice, and tumor volume was measured twice a week (0.5 × Length × Width^2, mm^3). The subcutaneous tumor and spleen were harvested from the mice for immunological assays 1-3 weeks after tumor implantation.

Functional analysis of CD11b^{+} cells

CD11b^{+} cells were sorted from spleen cells (SPCs) of naive mice or tumor-implanted mice (day 14), or PBMCs obtained from healthy donors using a BD IMag system (BD Biosciences) with magnetic particle-conjugated anti-CD11b mAb (BD Biosciences) according to the manufacturer's instructions. The sorted CD11b^{+} cells were cultured in 10% FBS/RPMI1640 for 2 hrs, and the adherent cells were isolated as CD11b^{+} myeloid cells. The naive CD11b^{+} cells were stimulated with FSTL1 (10 ng/ml; R&D) in the presence or absence of anti-FSTL1 mAb, anti-LAG3 mAb, or rat IgG (R&D) as a control, and were analyzed by flow cytometry. To assess the immunomodulatory effect on T cells, the CD11b^{+} cells were cocul-

tured (2:1) with CD3+ or CD8+ T cells sorted from mouse SPCs or human PBMCs in the presence of anti-CD3 mAb (BD Biosciences) along with anti-LAG3 mAb (1 μg/ml; Clone C9B7W, BioXCell) or rat IgG as a control. Three to five days later, the CD3+ cells were analyzed for annexin V+ apoptotic cells by flow cytometry. For tracking cell division, the CD8+ T cells were labeled with CFSE before the coculture. In a setting, the CD11b+ cells were treated with tumor supernatants for 3-5 days before assays. In the in vivo assay, the CD11b+ cells (3×10^5) were s.c. coinjected with tumor cells (3×10^5) in mice, and anti-LAG3 mAb or rat IgG (10 mg/kg) were intraperitoneally (i.p.) injected in the mice. The subcutaneous tumor and spleen were harvested from the mice for immunological assays 3 weeks after tumor implantation.

In vivo therapy

C57BL/6 mice were s.c. implanted with MC38 cells (5×10^5), and were i.p. injected with anti-LAG3 mAb, anti-PD1 mAb (Clone 29F.1A12; BioLegend), or rat IgG as a control at 10 mg/kg on days 4 and 7 after tumor implantation. To evaluate CTL induction in the treated mice, spleen cells were firstly stimulated with a tumor antigen gp70 peptide (1 μg/mL) for 6 days, and then the recovered CD8+ T cells (2×10^5 cells) were tested for the cytotoxic activity (target = MC38 parental cells, E:T ratio = 20:1, 4 hrs) using the Immunocyto Cytotoxicity Detection kit (MBL) according to the manufacturer's instructions. To evaluate the anti-tumor efficacy of the treatment regimen in genetically unmodified tumor models, we used BALB/c mice that Colon26 cells were both s.c. (3×10^5 cells) and intravenously (i.v.; 3×10^5 cells) implanted mimicking metastatic cancer patients. The mice were i.p. injected with anti-LAG3 mAb, anti-FSTL1 mAb that we established before [11], or rat IgG (5 mg/kg) as a control on days 4 and 7. The s.c. tumors, lung, and spleen were harvested from the mice for assays 2-3 weeks after tumor implantation. Tumor metastatic nodules in lungs were counted after fixation with Fekete's solution.

Flow cytometric analysis

After Fc blocking, cells were stained with the following immunofluorescence-conjugated antibodies in mouse study: anti-CD45-APC (BD Biosciences), anti-CD3e-APC (BD), anti-CD3e-FITC (BD), anti-CD3e-PerCP/Cy5.5 (BD), anti-CD8a-PE (BD), ant-CD8a-PE/Cy5 (BioLegend), anti-CD11b-FITC (BioLegend), anti-CD11b-PerCP/Cy5.5 (BioLegend), anti-Gr1-PE (BioLegend), anti-PD1-FITC (BioLegend), anti-annexin V-PE (BD), anti-DIP2A-FITC (Bioss), anti-LAG3-PE (BioLegend), anti-Eomes-PE (Invitrogen), anti-TIM3-Alexa 488 (R&D), anti-TIGIT-PE (BioLegend), or the appropriate isotype control. Data were acquired using the FACSCalibur cytometer (BD), and were analyzed by Cellquest software (BD). In clinical study, the following antibodies were used: anti-CD45-APC-Cy7 (BioLegend), anti-CD3-BUV496 (BD), anti-CD8-BUV395 (BD), anti-Ki67-FITC (BioLegend), anti-GZMB-PE-Cy7 (BioLegend), anti-CD11b-BV510 (BioLegend), anti-DIP2A (Bioss), anti-LAG3 (BioLegend), or the appropriate isotype control. For intracellular staining, cells were treated with Cytofix/Cytoperm solution (BD) before antibody staining. Data were acquired using a BD LSR Fortessa X-20 cytometer (BD), and were analyzed by FlowJo software (BD). Before defining the specific molecular expressions, debris was firstly excluded by FSC/SSC, and immunofluorescence intensity was compared to the isotype control.

Clinical analysis

For immunohistochemical analysis, we used tumor tissues surgically resected from patients with stage I-IV CRC at National Cancer Center Hospital East (June 2010-January 2012), according to the protocol approved by the Institutional Review Board of the National Cancer Center (n = 306; **Table 1**). No patients received systemic chemotherapy before surgery. We stained the paraffin-embedded tumor sections with the following antibodies as described before [11]: anti-DIP2A-FITC (Bioss), anti-FSTL1-PE, anti-LAG3-PE (R&D), anti-CD8-FITC (BD), or the isotype IgG (BioLegend). The immunofluorescence intensity was automatically measured as pixel counts at two fields per section using a LSM700 Laser Scanning Microscope (Carl Zeiss), and the average was used in graphs. The mean pixels stained with isotype control (background) were FSTL1 0.5×10^4 and DIP2A 2×10^4. The mean pixels in normal tissues were FSTL1 1.8×10^4 and DIP2A 3.2×10^4 (mean normal), and the mean pixels in tumor tissues were FSTL1 2.3×10^4 and DIP2A 7.1×10^4 (mean tumor). The molecular expression patterns were categorized into 4 levels: Level 0, less than background (no expression); Level 1, more than background

Table 1. Demographics of colorectal cancer patients and the statistical association with FSTL1/DIP2A expressions in the tumor tissues

Characteristics (n = 306)	
Median age (range)	FSTL1, P = 0.729; DIP2A, P = 0.795
	65 (26-85)
Sex	FSTL1, P = 0.496; DIP2A, P = 0.897
Male	172 (56.2%)
Female	134 (43.8%)
Pathological stage	FSTL1, P = 0.195; DIP2A, P = 0.857
1	64 (20.9%)
2	105 (34.3%)
3	97 (31.7%)
4	40 (13.1%)
Tumor depth	FSTL1, P = 0.566; DIP2A, P = 0.148
1	22 (7.2%)
2	59 (19.3%)
3	180 (58.8%)
4	45 (14.7%)
Lymph node metastasis	FSTL1, P = 0.783; DIP2A, P = 0.802
0	182 (59.5%)
1	88 (28.8%)
2	36 (11.8%)

but less than mean normal (weak expression); Level 2, more than mean normal d but less than mean tumor (moderate expression); Level 3, more than mean tumor (strong expression). For flow cytometry analysis, PBMCs were isolated from EDTA-added peripheral blood obtained from healthy donors (n = 4; 40-43 years old) and patients with stage IV metastatic CRC (n = 11; 57-79 years old; male = 7, female = 4) at National Cancer Center Hospital (November 2018-January 2020) according to the protocol approved by the Institutional Review Board of the National Cancer Center. The plasma was tested for FSTL1 using an ELISA kit (R&D). All activities were conducted in accordance with the ethical principles of the Declaration of Helsinki.

Statistical analysis

Data indicate means ± SDs unless otherwise specified. Significant differences (*P* value < 0.05) were statistically evaluated using GraphPad Prism 7 software (MDF) or SPSS Statistics 23.0 software (IBM). Data between two groups were analyzed by the unpaired two-tailed Student's t test. Data among multiple groups were analyzed by one-way ANOVA, followed by the Bonferroni post-hoc test for pairwise comparison of groups based on the normal distributions. Non-parametric groups were analyzed by the Mann-Whitney test, the Jonckheere-Terpstra test, and the Chi-squared test. Survival of mice and patients was analyzed by the Kaplan-Meier method and ranked according to the Mantel-Cox log-rank test. Correlation between two factors was evaluated by the nonparametric Spearman's rank test.

Results

Apoptotic T cells increase in the mice with FSTL1$^+$ colorectal cancer

To clearly examine the influences of CRC-derived FSTL1, we firstly established FSTL1 transfectants using murine CRC FSTL1$^{-/low}$ MC38 cells. The FSTL1 transfectants (designated TR) showed a significantly higher invasive property, but significantly lower proliferative and adhesive property as compared to mock transfectant (P < 0.05; **Figure 1A**). In vivo growth of the TR tumors was also significantly slower than the mock growth after subcutaneous (s.c.) implantation in mice (P < 0.0004; **Figure 1B**). These suggest FSTL1 overexpression confers EMT-like properties on tumor cells as reported elsewhere [13, 14]. In the TR tumors, CD3$^+$ T cells temporally but abundantly increased (P = 0.019 versus mock on day 14), but were apoptotic expressing annexin V and PD1 followed by marked decrease in a week (P = 0.0001 versus mock on day 21; **Figure 1C**). Apoptotic T cells also significantly increased in spleen of the TR-implanted mice (P = 0.018 versus mock on day 14), and CD8 intensity that is important for T-cell activation was downregulated in the cells (**Figure 1D**). This suggests that local FSTL1 expression in tumors systemically damages anti-tumor immunity in the host. These results are consistent with previous data using other tumor models [18]. In the present study, however, we additionally found significant increase of a subset expressing a FSTL1 receptor DIP2A and an IC molecule LAG3 in splenic CD11b$^+$Gr1$^+$ myeloid cells of the TR-implanted mice (P < 0.0001 versus mock; **Figure 1E**). This raised a question of whether the increased CD11b$^+$DIP2A$^+$LAG3$^+$ cells might be involved in the T-cell exclusion mechanisms.

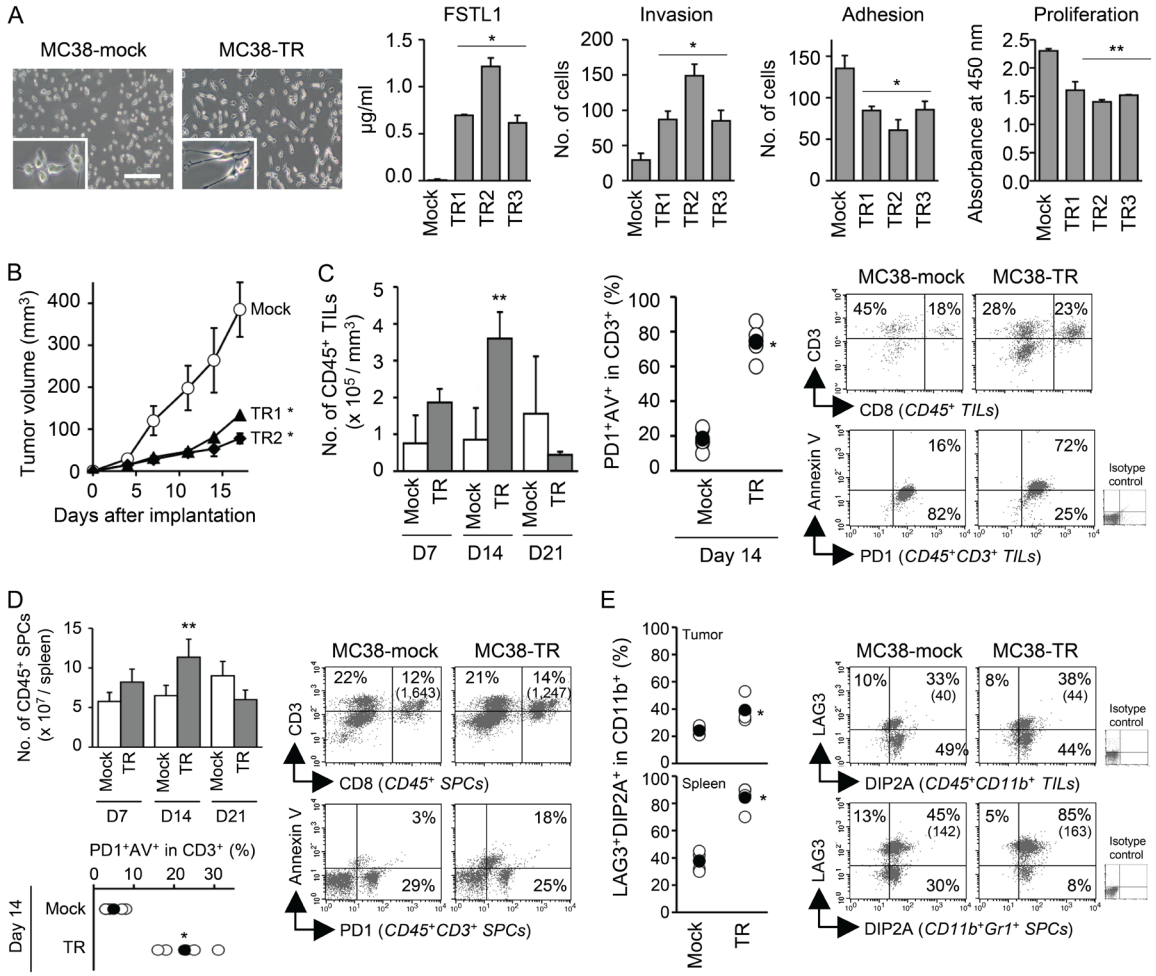

Figure 1. Apoptotic T cells increase in the mice with FSTL1⁺ colorectal cancer. A. Establishment of FSTL1 transfectants (TR1-3) using murine colorectal cancer (CRC) MC38 cells. Photos show morphological changes (round types to spindle types) after *fstl1* transduction (scale = 1,000 μm). FSTL1 in the cultured supernatants was measured by ELISA, and cellular functions were tested (n = 3). B. Retardation of the TR tumor growth after subcutaneous implantation in mice (n = 5). C. Increase of PD1⁺ annexin V⁺ apoptotic T cells within the TR tumors (day 14; n = 5). D. Increase of PD1⁺ annexin V⁺ apoptotic T cells in spleen of the TR-implanted mice (day 14; n = 5). E. Expansion of a DIP2A⁺LAG3⁺ subset in the CD11b⁺ cells of the TR-implanted mice (day 14; n = 5). Graphs show means ± SDs except scatter plots (open circles, individual data; closed circles, means). *P < 0.01, **P < 0.05 versus mock control. Representative data of three independent experiments.

The T-cell apoptosis is caused by the FSTL1⁺ tumor-induced CD11b⁺DIP2A⁺LAG3⁺ cells

When naive CD11b⁺ cells were stimulated with FSTL1, LAG3 expression was upregulated, and the LAG3 upregulation was abrogated by anti-FSTL1 mAb (**Figure 2A**). This suggests that the CD11b⁺LAG3⁺ cells expansion in the TR-implanted mice are possibly induced by the tumor-derived FSTL1. Then, we characterized the CD11b⁺ cells containing the DIP2A⁺LAG3⁺ subset sorted from SPCs of the TR-implanted mice (designated TR-CD11b⁺). When CD8⁺ T cells were cocultured with the TR-CD11b⁺ cells in the presence of anti-CD3 mAb for 3-5 days, cell proliferation was significantly suppressed potentially via apoptosis induction, although CD11b⁺ cells sorted from the mock-implanted mice (designated mock-CD11b⁺) stimulated the cell proliferation (P = 0.0003 versus no CD11b⁺ cells; **Figure 2B**). In the TR-CD11b⁺-cocultured CD8⁺ T cells, IC molecular expressions were markedly enhanced, suggesting induction of immune exhaustion (**Figure 2C**). The CD8 intensity that is important for T-cell activation was extremely reduced as compared to those of CD8⁺ T cells cocultured with mock-CD11b⁺ cells (**Figure 2C**). When MC38 parental cells were s.c. coinjected with the TR-CD11b⁺ cells, tumor growth was markedly

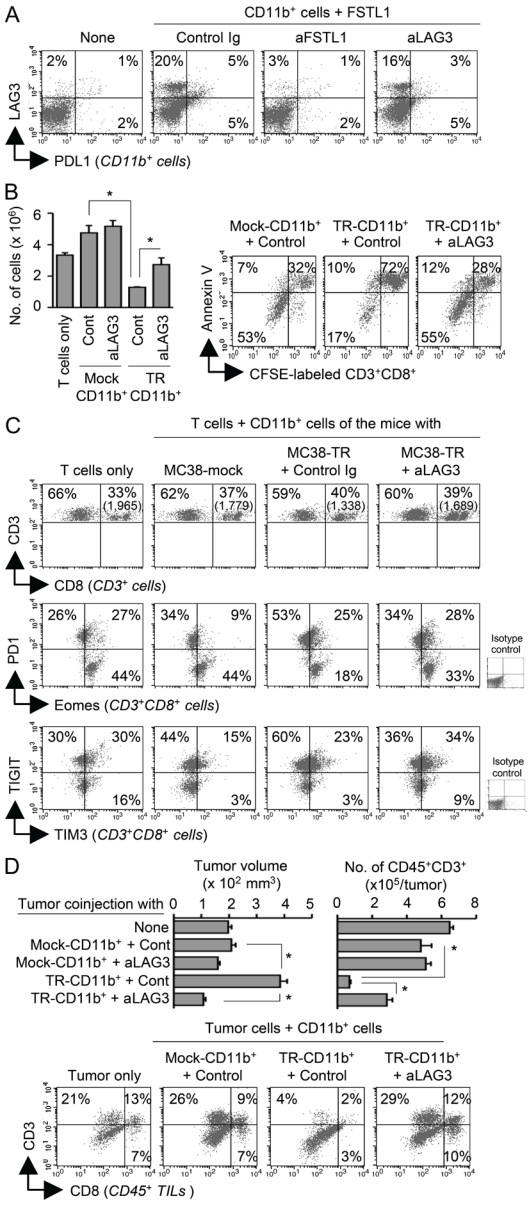

Figure 2. The T-cell apoptosis is caused by the FSTL1$^+$ tumor-induced CD11b$^+$DIP2A$^+$LAG3$^+$ cells. (A) FSTL1 upregulates LAG3 expression in CD11b$^+$ cells. Splenic CD11b$^+$ cells obtained from naive mice were stimulated with FSTL1 in the presence or absence of anti-FSTL1 mAb, anti-LAG3 mAb, or isotype control for 3 days, and were analyzed by flow cytometry. (B, C) The TR-stimulated CD11b$^+$ cells suppress CD8$^+$ T-cell proliferation partly via LAG3. Splenic CD11b$^+$ cells obtained from tumor-implanted mice (day 14) were cocultured (2:1) with CD8$^+$ T cells (2:1) in the presence of anti-CD3 mAb and/or anti-LAG3 mAb for 5 days (n = 3). CFSE-labeled CD8$^+$ T cells were used for tracking cell division (B). The cocultured CD8$^+$ T cells were analysed for expression of immune checkpoint molecules by flow cytometry (C). (D) In vivo T-cell exclusion caused by the TR-stimulated CD11b$^+$ cells partly via the LAG3. MC38 cells were s.c. coinjected (1:1) with the CD11b$^+$ cells in mice, and 4 days later, the mice were treated with anti-LAG3 mAb or isotype control at 10 mg/kg (n = 5). Twenty days after coinjection, tumors and spleens were harvested for flow cytometric analysis. *P < 0.01, **P < 0.05. Graphs show means ± SDs. Representative data of three independent experiments.

facilitated following rare immune infiltration (P = 0.003 versus no CD11b$^+$ cells; **Figure 2D**). These suggest that the TR-CD11b$^+$ cells play a key role in the T-cell exclusion potentially via apoptosis. Interestingly, blocking LAG3 with the specific mAb partly but significantly rescued from the TR-CD11b$^+$-caused adverse events (P < 0.01 versus control), although no effect was seen in the tumors coinjected with mock-CD11b$^+$ cells (**Figure 2**). This suggests that LAG3 that is possibly expressed in the CD11b$^+$ myeloid cells is partly involved in the mechanisms, although we have to also take account of LAG3 expressed in T cells.

We validated the findings in human system using human CRC HCT116 cells transduced with human *fstl1*. FSTL1 transduction confers EMT-like properties on tumor cells as seen in mouse MC38 cells (**Figure 3A**). When CD11b$^+$ cells sorted from human PBMCs were stimulated with the TR-cultured supernatants for 5 days, the DIP2A$^+$LAG3$^+$ subset was expanded, and the increase was markedly suppressed by blocking FSTL1 with the specific mAb that we established before [11], suggesting involvement of FSTL1 (**Figure 3B**). When CD3$^+$ T cells were cocultured with the TR-stimulated CD11b$^+$ cells in the presence of anti-CD3 mAb for 5 days, cell proliferation was only slightly enhanced (P = 0.240 versus no CD11b$^+$ cells), although mock-stimulated CD11b$^+$ cells strongly enhanced the cell proliferation (P = 0.0125; **Figure 3B**). Addition of anti-LAG3 mAb to the cocultured with the TR-stimulated CD11b$^+$ cells remarkably enhanced the cell proliferation (P = 0.028 versus control), although no effect of anti-LAG3 addition was seen in the cocultured with the mock-stimulated CD11b$^+$ cells (**Figure 3B**). These suggest the close relationship among CRC-derived FSTL1, increase of CD11b$^+$DIP2A$^+$LAG3$^+$ cells, and T-cell dysfunction in human settings.

Blocking FSTL1 and LAG3 synergizes in treatment of mouse CRC models

Anti-PD1 therapy were ineffective in the TR-implanted mice (P = 0.233 versus control; **Figure 4A**). In these mice, although expansion

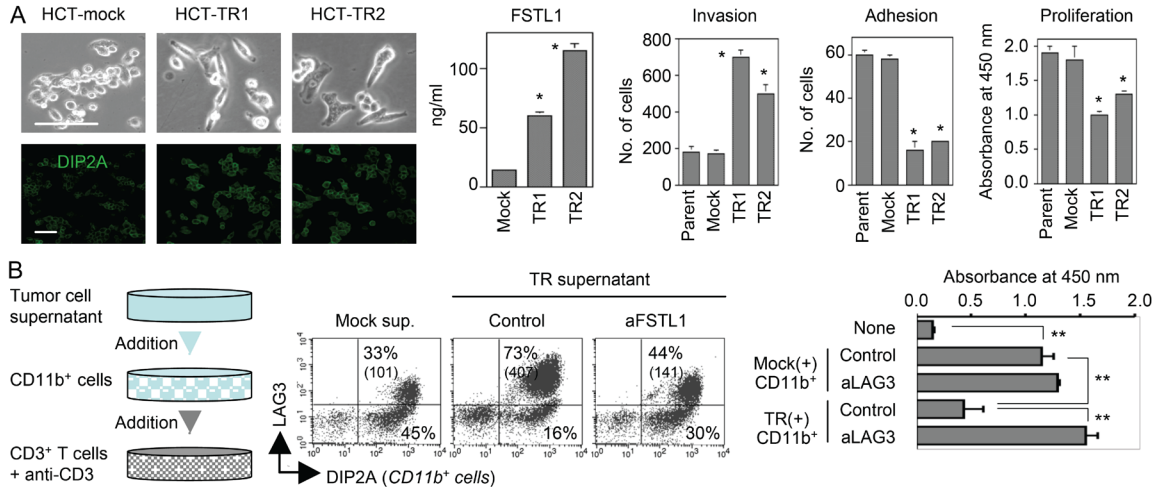

Figure 3. Blocking LAG3 interferes the FSTL1-induced T-cell suppression in human system. A. Establishment of FSTL1 transfectants (TR1-3) using human CRC HCT116 cells. Photos show morphological changes (round types to spindle types) and DIP2A enhancement after *fstl1* transduction (scale = 100 μm). FSTL1 in the cultured supernatants was measured by ELISA, and cellular functions were tested (n = 3). *P < 0.01 versus mock control. B. The TR-induced CD11b⁺ cells suppress T-cell proliferation via LAG3. CD11b⁺ were sorted from human PBMCs, and were stimulated with tumor supernatant fluids for 5 days followed by flow cytometric analysis for LAG3 and DIP2A expressions. CD3⁺ T cells were cocultured (2:1) with the stimulated CD11b⁺ cells in the presence of anti-CD3 mAb and/or anti-LAG3 mAb for 5 days (n = 3). **P < 0.05. Graphs show means ± SDs. Representative data of two independent experiments.

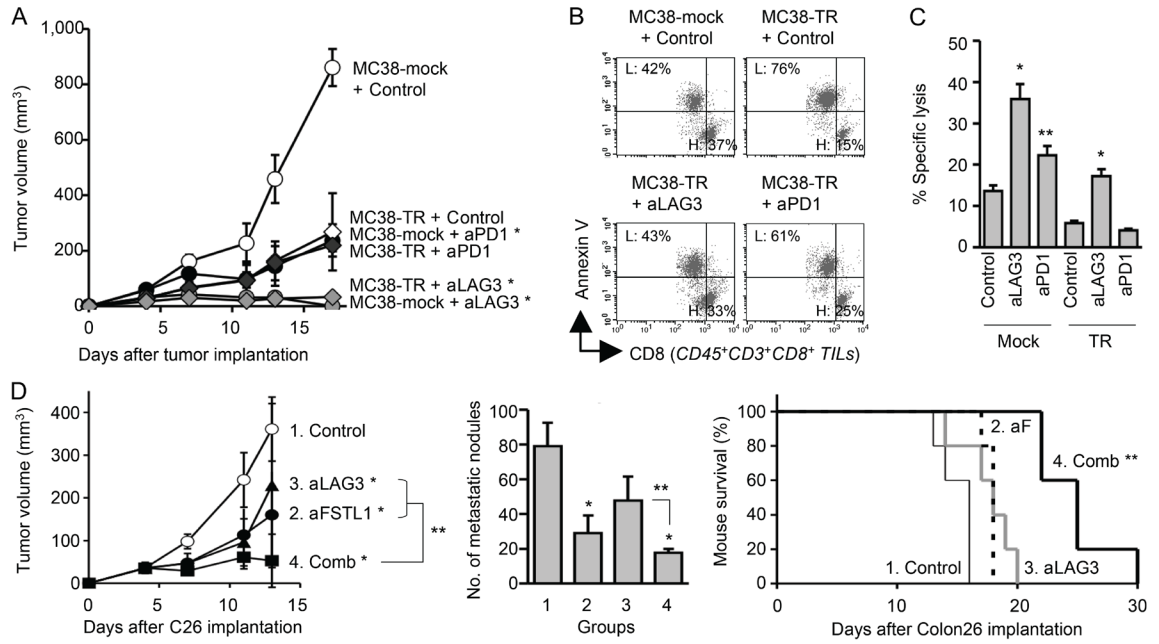

Figure 4. Blocking FSTL1 and LAG3 synergizes in treatment of mouse CRC models. (A-C) Blocking LAG3 successfully elicits anti-tumor effects by suppressing CD8⁺ T-cell apoptosis in the TR-implanted mice. Mice were s.c. implanted with tumor cells, and were i.p. injected with anti-PD1 mAb, anti-LAG3 mAb, or rat IgG as a control (10 mg/kg) on days 4 and 7 after tumor implantation (n = 5). Tumor growth was measured (A), and tumors and spleen were harvested for flow cytometric analysis (B) and cytotoxic assay (E:T ratio = 20:1; C) on day 18. (D) Blocking LAG3 synergizes with blocking FSTL1 in the treatment of CRC metastasis models. Mice were both s.c. and intravenously (i.v.) implanted with FSTL1⁺ Colon26 cells, and were i.p. injected with anti-LAG3 mAb, anti-FSTL1 mAb, and/or rat IgG (5 mg/kg) on days 4 and 7 (n = 5). *P < 0.01, **P < 0.05 versus control group. Graphs show means ± SDs. Representative data of three independent experiments.

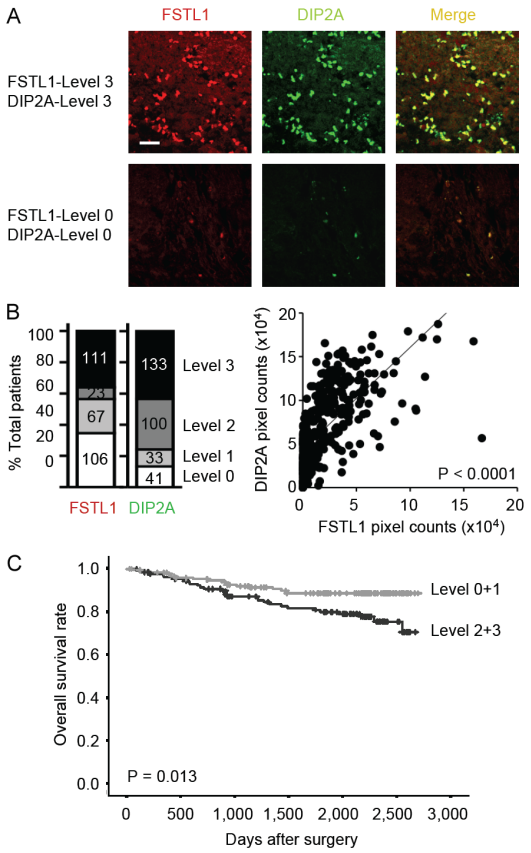

Figure 5. FSTL1 positivity in tumor tissues significantly correlates with poor prognosis of CRC patients. Tumor tissues obtained from CRC patients were immunohistochemically analyzed for FSTL1 and DIP2A expressions (n = 306). A. Representative photos (scale = 100 μm). B. Significant correlation between FSTL1 and DIP2A expressions. The molecular expression patterns were categorized into 4 levels according to the immunofluorescence intensity depicted as pixel counts: Level 0, no expression; Level 1, weak expression; Level 2, moderate expression; and Level 3, strong expression. C. FSTL1 positivity is reversely correlated with overall survival of the patients.

of apoptotic T cells was slightly suppressed (**Figure 4B**), cytotoxic activity of the CTLs was not elevated (**Figure 4C**). In contrast, anti-LAG3 therapy induced potent CTLs with much higher cytotoxic activity, and the TR tumor growth was significantly suppressed in the mice (P = 0.004: **Figure 4A-C**). Anti-LAG3 therapy also significantly suppressed tumor growth (P 0.029) and metastasis (P = 0.032) in the Colon26 metastasis models (**Figure 4D**), although anti-PD1 therapy was ineffective as shown before [11]. However, the impact was small on mouse survival (P = 0.075). Anti-FSTL1 therapy was also effective in this tumor model, and significantly enhanced the anti-LAG3 efficacy, resulting in significant better prognosis of the mice (P < 0.01 versus monotherapy; **Figure 4D**). These suggest that blocking FSTL1 and LAG3 successfully elicits potent anti-tumor immunity in the hosts with FSTL1⁺ CRC.

Clinical relevancy of CD11b⁺DIP2A⁺LAG3⁺ cell expansion in CRC

We finally validated the clinical relevancy of the basic findings. FSTL1 expression was upregulated in 43% (Level 2 + 3) of tumor tissues obtained from CRC patients (n = 306; **Table 1**; **Figure 5A** and **5B**), and the positivity was reversely and significantly correlated with overall survival of the patients (P = 0.013; **Figure 5C**), as shown in elsewhere [13, 14]. No significant relationships with other clinicopathological features, such as staging and metastasis, were seen. DIP2A expression was also upregulated in 76% of tumor tissues, and the intensity was significantly correlated with the FSTL1 intensity (P < 0.0001; **Figure 5B**). No significant correlation was seen between DIP2A expression and the clinicopathological features. DIP2A was mostly expressed in FSTL1⁺ tumor cells, although the total intensity was composed of all cells, including tumor cells, stromal cells, and immune cells by full scan. Evaluation of LAG3 expression was impossible because of the limitation of the specimens. We also analyzed peripheral blood obtained from stage IV metastatic CRC patients (n = 11) and healthy donors (n = 4). FSTL1 was significantly increased in the peripheral blood of the patients as compared to that of healthy donors (P = 0.006; **Figure 6A**), and a DIP2A⁺LAG3⁺ subset was expanded in the CD11b⁺ PBMCs (P = 0.048 versus Healthy; **Figure 6B**, **6C**). In the patients, CD3⁺CD8⁺Ki67⁺GZMB⁺ T cells were markedly reduced (P = 0.025), and the decrease was significantly correlated with increase of the CD11b⁺DIP2A⁺LAG3⁺ cells (P = 0.005; **Figure 6C**). These show the clinical relevancy of the basic findings. Collectively, targeting FSTL1 along with LAG3 may be a promising strategy for treating metastatic CRC in the clinical settings.

Discussion

In this study, we uncover the immunological mechanisms caused by CRC-derived FSTL1.

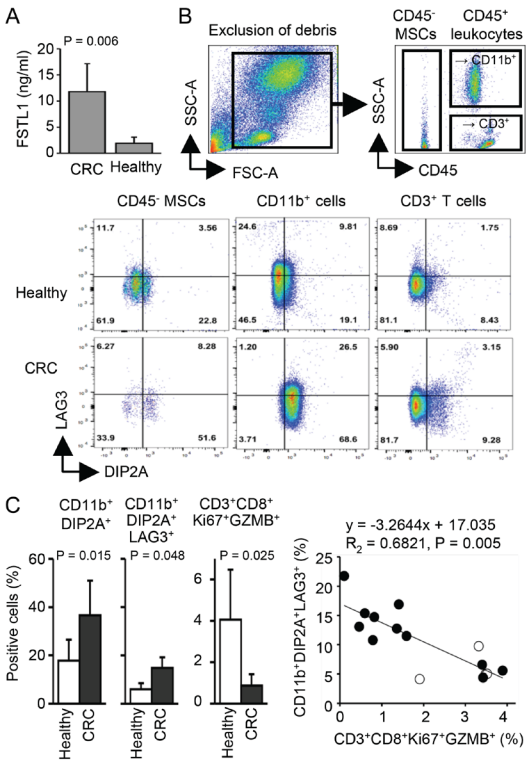

Figure 6. CD11b+DIP2A+LAG3+ cells are expanded in peripheral blood of metastatic CRC patients. PBMCs were obtained from healthy donors (n = 4) and patients with stage IV metastatic CRC (n = 11). A. FSTL1 concentration measured by ELISA (means ± SDs). B. Gating strategy and representative dot plot data in flow cytometric analysis. C. Significant correlation between CD11b+DIP2A+LAG3+ cell expansion and CD3+CD8+Ki67+GZMB+ T-cell reduction. Open circles, healthy donors. Closed circles, CRC patients. The *P* value in the scatter plot was analyzed by the non-parametric Spearman's rank test.

FSTL1+ tumor cells with EMT-like properties abundantly expand CD11b+DIP2A+LAG3+ myeloid cells, which induce apoptosis in T cells partly via LAG3 signaling leading to immune dysfunction. We confirmed in the in vitro settings that human FSTL1+ CRC cells expand CD11b+DIP2A+LAG3+ cells that are incompetent to stimulate T-cell proliferation. Blocking LAG3, however, suppresses the apoptosis induction in T cells, and successfully induces anti-tumor efficacy in the FSTL1+ tumor metastasis models. The anti-LAG3 therapy synergizes with anti-FSTL1 therapy in providing better prognosis in the mice. In metastatic CRC patients, FSTL1 is upregulated in tumor tissues and peripheral blood accompanied by expansion of the CD11b+DIP2A+LAG3+ cells and decrease of potent CTLs. Thus, targeting the FSTL1-LAG3 axis may be a promising strategy for treating metastatic CRC, and anti-FSTL1/LAG3 combination regimen may be practically useful in the clinical settings.

We previously demonstrated that tumor-derived FSTL1 induces immune exhaustion and dysfunction through expansion of activated mesenchymal stem cells (MSCs) [11, 18]. In the present study, we additionally identified another mechanism of immune dysfunction mediated by T-cell apoptosis caused by the FSTL1-induced CD11b+DIP2A+LAG3+ cells. This finding further deepens the understanding of the FSTL1 roles in cancer pathogenesis. CD45- MSCs partly expressing DIP2A and LAG3 were also expanded in mice and patients with FSTL1+ CRC as well as other tumor models in our previous studies [11, 18]. However, the proportion and the number of the CD11b+DIP2A+LAG3+ cells were absolutely larger than those of the MSCs, potentially giving much wider and stronger influences in the host. These suggest that the FSTL1-induced CD11b+DIP2A+LAG3+ cells are the key driver of immune dysfunction in metastatic CRC.

FSTL1 is known to regulate tumor progression and metastasis not only positively as a tumor facilitator as shown in our studies, but also negatively as a tumor suppressor followed by increase of tumor-infiltrating cells (TILs) [20, 21]. The discrepancy may depend on the differences of tumor cells, mouse models, or the broad range of biological actions of FSTL1. However, the tumor suppression induced by FSTL1 may be explainable by the low proliferative property conferred via the EMT program, and the increased TILs may be apoptotic and disappearing sometime after the sampling as shown in our study. Actually, TILs were rarely seen in the tumor tissues of many CRC patients.

LAG3 is an IC molecule involved in immune exhaustion and dysfunction, particularly of anti-tumor effector cells, such as T cells and NK cells, and thus targeting LAG3 has attracted attention as a promising strategy for reinvigorating these cells under cancer [22]. In our study, however, LAG3 expressed in myeloid cells was a key player in the immune dysfunction caused by FSTL1+ CRC, and was functionally critical for inducing apoptosis in T cells, although the detailed mechanisms should be elucidated. In addition, there were no differ-

ences of LAG3 expression in T cells between healthy donors and CRC patients. LAG3 expression has been shown in other cells, such as B cells [23, 24], plasmacytoid dendritic cells [25], and macrophages [24], although the cellular functions remain unclear. LAG3 has several receptors/ligands [26], and some of them such as galectin 3 [27] and CLEC4G [28] are associated with T-cell dysfunction and apoptosis. These molecules may be involved in the T-cell apoptosis mechanism shown in this study. The details should be defined in the further studies

Anti-LAG3 mAbs have been developed in combination with other agents for treating various types of cancer, although the evaluation is still underway [22]. FSTL1 blockade may be useful for boosting the therapeutic activity, particularly in the treatment of metastatic CRC. Anti-PD1/PDL1 mAbs have been favorably combined with anti-LAG3 mAbs in many clinical trials [29, 30]. However, it will be necessary to change the therapeutic strategy based on the scientific evidence. Anti-FSTL1 therapy may be one of the better choices to enhance the anti-LAG3 efficacy, and FSTL1 expression in tumors may be useful for predicting potential unresponsiveness to the anti-PD1/PDL1 therapy. Thus, this study provides a rationale of targeting FSTL1 along with LAG3 in the treatment of metastatic CRC. To translate the findings to clinic, further studies using more clinical samples are needed to define the relationships with anti-PD1 responses and the related biomarkers, such as PDL1 expression, MSI, and mutation burden in tumor tissues.

Acknowledgements

This study was financially supported by the Japan Agency for Medical Research and Development P-CREATE, Tokyo, Japan (106209 to C.K.-S), and Pharma Foods International Co., Ltd., Kyoto, Japan. Authors' contributions: C.K.-S. conceptualized, designed and directed this study, conducted experiments, analyzed data, and wrote the manuscript. Y.O. conducted in vitro and in vivo experiments, and analyzed data. H.I. conducted experiments and clinical study, and analyzed data. Y.U. and R.Z. generated FSTL1 transfectants. A.K.-N. and M.K. conducted clinical study, and analyzed data. N.B. and A.O. supervised clinical study. The authors thank Takahiro Miyamoto for his excellent assistance in the clinical study, and thank Mami Kawamura for her excellent assistance in the in vivo study.

Disclosure of conflict of interest

None.

Address correspondence to: Chie Kudo-Saito, Department of Immune Medicine, National Cancer Center Research Institute, Tokyo, Japan. E-mail: ckudo@ncc.go.jp

References

[1] Dekker E, Tanis PJ, Vleugels JLA, Kasi PM and Wallace MB. Colorectal cancer. Lancet 2019; 394: 1467-1480.

[2] Castagnoli L, De Santis F, Volpari T, Vernieri C, Tagliabue E, Di Nicola M and Pupa SM. Cancer stem cells: devil or savior-looking behind the scenes of immunotherapy failure. Cells 2020; 9: 555.

[3] Venook AP, Niedzwiecki D, Lenz HJ, Innocenti F, Fruth B, Meyerhardt JA, Schrag D, Greene C, O'Neil BH, Atkins JN, Berry S, Polite BN, O'Reilly EM, Goldberg RM, Hochster HS, Schilsky RL, Bertagnolli MM, El-Khoueiry AB, Watson P, Benson AB 3rd, Mulkerin DL, Mayer RJ and Blanke C. Effect of first-line chemotherapy combined with cetuximab or bevacizumab on overall survival in patients with kras wild-type advanced or metastatic colorectal cancer: a randomized clinical trial. JAMA 2017; 317: 2392-2401.

[4] Venderbosch S, Nagtegaal ID, Maughan TS, Smith CG, Cheadle JP, Fisher D, Kaplan R, Quirke P, Seymour MT, Richman SD, Meijer GA, Ylstra B, Heideman DA, de Haan AF, Punt CJ and Koopman M. Mismatch repair status and BRAF mutation status in metastatic colorectal cancer patients: a pooled analysis of the CAIRO, CAIRO2, COIN, and FOCUS studies. Clin Cancer Res 2014; 20: 5322-5330.

[5] Le DT, Uram JN, Wang H, Bartlett BR, Kemberling H, Eyring AD, Skora AD, Luber BS, Azad NS, Laheru D, Biedrzycki B, Donehower RC, Zaheer A, Fisher GA, Crocenzi TS, Lee JJ, Duffy SM, Goldberg RM, de la Chapelle A, Koshiji M, Bhaijee F, Huebner T, Hruban RH, Wood LD, Cuka N, Pardoll DM, Papadopoulos N, Kinzler KW, Zhou S, Cornish TC, Taube JM, Anders RA, Eshleman JR, Vogelstein B and Diaz LA Jr. PD-1 blockade in tumors with mismatch-repair deficiency. N Engl J Med 2015; 372: 2509-2520.

[6] Le DT, Kim TW, Van Cutsem E, Geva R, Jager D, Hara H, Burge M, O'Neil B, Kavan P, Yoshino T, Guimbaud R, Taniguchi H, Elez E, Al-Batran SE, Boland PM, Crocenzi T, Atreya CE, Cui Y, Dai T, Marinello P, Diaz LA Jr and Andre T. Phase II

open-label study of pembrolizumab in treatment-refractory, microsatellite instability-high/mismatch repair-deficient metastatic colorectal cancer: KEYNOTE-164. J Clin Oncol 2020; 38: 11-19.
[7] Anderson AC, Joller N and Kuchroo VK. Lag-3, Tim-3, and TIGIT: co-inhibitory receptors with specialized functions in immune regulation. Immunity 2016; 44: 989-1004.
[8] Bluthgen MV, Baste N and Recondo G. Immunotherapy combinations for the treatment of patients with solid tumors. Future Oncol 2020; 16: 1715-1736.
[9] Lau MC, Ng KY, Wong TL, Tong M, Lee TK, Ming XY, Law S, Lee NP, Cheung AL, Qin YR, Chan KW, Ning W, Guan XY and Ma S. FSTL1 promotes metastasis and chemoresistance in esophageal squamous cell carcinoma through NFkappaB-BMP signaling cross-talk. Cancer Res 2017; 77: 5886-5899.
[10] Yang W, Wu Y, Wang C, Liu Z, Xu M and Zheng X. FSTL1 contributes to tumor progression via attenuating apoptosis in a AKT/GSK-3beta-dependent manner in hepatocellular carcinoma. Cancer Biomark 2017; 20: 75-85.
[11] Kudo-Saito C, Ishida A, Shouya Y, Teramoto K, Igarashi T, Kon R, Saito K, Awada C, Ogiwara Y and Toyoura M. Blocking the FSTL1-DIP2A axis improves anti-tumor immunity. Cell Rep 2018; 24: 1790-1801.
[12] Nie E, Miao F, Jin X, Wu W, Zhou X, Zeng A, Yu T, Zhi T, Shi Z, Wang Y, Zhang J, Liu N and You Y. Fstl1/DIP2A/MGMT signaling pathway plays important roles in temozolomide resistance in glioblastoma. Oncogene 2019; 38: 2706-2721.
[13] Gu C, Wang X, Long T, Wang X, Zhong Y, Ma Y, Hu Z and Li Z. FSTL1 interacts with VIM and promotes colorectal cancer metastasis via activating the focal adhesion signalling pathway. Cell Death Dis 2018; 9: 654.
[14] Zhao Y, Ou Q, Deng Y, Peng J, Li C, Li J, Zhao Q, Qiu M, Wan D, Fang Y and Pan Z. Determination of follistatin-like protein 1 expression in colorectal cancer and its association with clinical outcomes. Ann Transl Med 2019; 7: 606.
[15] Cogdill AP, Andrews MC and Wargo JA. Hallmarks of response to immune checkpoint blockade. Br J Cancer 2017; 117: 1-7.
[16] Kudo-Saito C, Ozaki Y, Imazeki H, Hayashi H, Masuda J, Ozawa H and Ogiwara Y. Targeting oncoimmune drivers of cancer metastasis. Cancers (Basel) 2021; 13: 554.
[17] Zhang R, Liu TY, Senju S, Haruta M, Hirosawa N, Suzuki M, Tatsumi M, Ueda N, Maki H, Nakatsuka R, Matsuoka Y, Sasaki Y, Tsuzuki S, Nakanishi H, Araki R, Abe M, Akatsuka Y, Sakamoto Y, Sonoda Y, Nishimura Y, Kuzushima K and Uemura Y. Generation of mouse pluripotent stem cell-derived proliferating myeloid cells as an unlimited source of functional antigen-presenting cells. Cancer Immunol Res 2015; 3: 668-677.
[18] Kudo-Saito C, Fuwa T, Murakami K and Kawakami Y. Targeting FSTL1 prevents tumor bone metastasis and consequent immune dysfunction. Cancer Res 2013; 73: 6185-6193.
[19] Kudo-Saito C, Shirako H, Takeuchi T and Kawakami Y. Cancer metastasis is accelerated through immunosuppression during Snail-induced EMT of cancer cells. Cancer Cell 2009; 15: 195-206.
[20] Chan QK, Ngan HY, Ip PP, Liu VW, Xue WC and Cheung AN. Tumor suppressor effect of follistatin-like 1 in ovarian and endometrial carcinogenesis: a differential expression and functional analysis. Carcinogenesis 2009; 30: 114-121.
[21] Ni X, Cao X, Wu Y and Wu J. FSTL1 suppresses tumor cell proliferation, invasion and survival in non-small cell lung cancer. Oncol Rep 2018; 39: 13-20.
[22] Puhr HC and Ilhan-Mutlu A. New emerging targets in cancer immunotherapy: the role of LAG3. ESMO Open 2019; 4: e000482.
[23] Kisielow M, Kisielow J, Capoferri-Sollami G and Karjalainen K. Expression of lymphocyte activation gene 3 (LAG-3) on B cells is induced by T cells. Eur J Immunol 2005; 35: 2081-2088.
[24] Keane C, Law SC, Gould C, Birch S, Sabdia MB, Merida de Long L, Thillaiyampalam G, Abro E, Tobin JW, Tan X, Xu-Monette ZY, Young KH, Gifford G, Gabreilli S, Stevenson WS, Gill A, Talaulikar D, Jain S, Hernandez A, Halliday SJ, Bird R, Cross D, Hertzberg M and Gandhi MK. LAG3: a novel immune checkpoint expressed by multiple lymphocyte subsets in diffuse large B-cell lymphoma. Blood Adv 2020; 4: 1367-1377.
[25] Workman CJ, Wang Y, El Kasmi KC, Pardoll DM, Murray PJ, Drake CG and Vignali DA. LAG-3 regulates plasmacytoid dendritic cell homeostasis. J Immunol 2009; 182: 1885-1891.
[26] Solinas C, Migliori E, De Silva P and Willard-Gallo K. LAG3: the biological processes that motivate targeting this immune checkpoint molecule in human cancer. Cancers (Basel) 2019; 11: 1213.
[27] Hsu DK, Yang RY and Liu FT. Galectins in apoptosis. Methods Enzymol 2006; 417: 256-273.
[28] Geijtenbeek TB and Gringhuis SI. Signalling through C-type lectin receptors: shaping immune responses. Nat Rev Immunol 2009; 9: 465-479.
[29] Matsuzaki J, Gnjatic S, Mhawech-Fauceglia P, Beck A, Miller A, Tsuji T, Eppolito C, Qian F, Lele S, Shrikant P, Old LJ and Odunsi K. Tumor-infiltrating NY-ESO-1-specific CD8+ T cells are neg-

atively regulated by LAG-3 and PD-1 in human ovarian cancer. Proc Natl Acad Sci U S A 2010; 107: 7875-7880.

[30] Woo SR, Turnis ME, Goldberg MV, Bankoti J, Selby M, Nirschl CJ, Bettini ML, Gravano DM, Vogel P, Liu CL, Tangsombatvisit S, Grosso JF, Netto G, Smeltzer MP, Chaux A, Utz PJ, Workman CJ, Pardoll DM, Korman AJ, Drake CG and Vignali DA. Immune inhibitory molecules LAG-3 and PD-1 synergistically regulate T-cell function to promote tumoral immune escape. Cancer Res 2012; 72: 917-927.